

Direct Detection of the Millicharged Background

Ella Iles,¹ Saniya Heeba,¹ and Katelin Schutz¹

¹*Department of Physics & Trottier Space Institute,
McGill University, Montréal, Québec H3A 2T8, Canada*

We show that dark matter direct detection experiments are sensitive to the existence of particles with a small effective charge (for instance, via couplings to a kinetically mixed, low-mass dark photon). Our forecasts do *not* depend on these particles comprising a significant fraction of the dark matter. Rather, these experiments are sensitive to the irreducible abundance produced in the early universe through the freeze-in mechanism. We find that ongoing and proposed direct detection experiments will have world-leading sensitivity to effective charges $Q \sim 10^{-12}$ across nine orders of magnitude in mass, corresponding to a dark matter sub-fraction as low as $\sim 10^{-3}$.

Introduction.— The need for physics beyond the Standard Model (SM) – including an explanation for the existence of dark matter (DM) – strongly motivates the study of dark sectors that are only weakly coupled to the SM. One minimal example of such a sector is comprised of particles that are charged under a dark $U(1)'$ gauge group (see e.g. Refs. [1–5]). Kinetic mixing between the dark and SM gauge bosons through $\kappa F^{\mu\nu} F'_{\mu\nu}$ provides the weak coupling between this dark sector and the SM [6–8]. This dimension-four operator can originate from a range of UV scenarios, including string theory models where extended gauge sectors are ubiquitous [9–12]. For ultralight $U(1)'$ gauge bosons, the kinetic mixing can be rotated away such that the dark sector particles pick up a small effective electromagnetic charge (millicharge) under the SM $U(1)$ in the low-energy limit,

$$\mathcal{L} \supset eQ\bar{\chi}\gamma_{\mu}\chi A^{\mu} + \bar{\chi}(i\not{\partial} - m_{\chi})\chi, \quad (1)$$

where the Dirac fermion χ is a millicharged particle (MCP) with dark charge g_{χ} and millicharge $Q = \kappa g_{\chi}/e$.

These theoretical considerations have made MCPs and dark photons a key benchmark for a range of collider and astronomical searches. Sub-MeV MCPs and dark photons can be produced copiously in stellar interiors and supernovae, impacting stellar evolution and other observables [13–20] while colliders can employ missing energy and displaced vertex techniques to search for the production of MCPs and dark photons [21–24]. Meanwhile, if MCPs are additionally assumed to comprise the observed DM of our Universe with $\Omega_{\text{DM}}h^2 = 0.12$ [25], they also pose a key experimental target for ongoing DM direct detection searches including SENSEI [26] and DAMIC [27], as well as the proposed OSCURA experiment [28]. In fact, MCPs as DM are also one of the main theoretical motivations for new approaches to sub-MeV direct detection [29], for instance proposals involving direct deflection [30], polar materials (GaAs and Al_2O_3) [31, 32] (which can include a multiphonon response [33, 34] detectable with SPICE [35]), Dirac materials (ZrTe_5 , Yb_3PbO , and BNQ-TTF) [36, 37], doped semiconductors [38], or superconductors (Al SC) [39, 40].

As summarized in Fig. 1, in this *Letter* we point out that if MCPs exist as particle states in the spectrum, then some MCP abundance will inevitably be produced

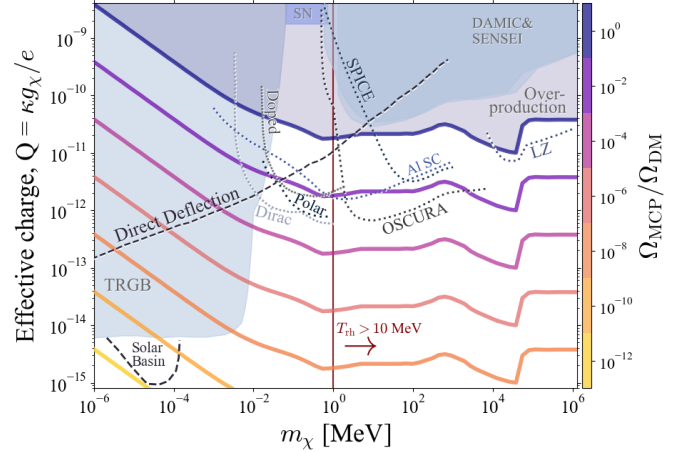


FIG. 1. Experimental reach of searches for MCPs. The solid lines represent the freeze-in relic abundance of MCPs normalized to the DM abundance. The shaded regions represent constraints from the TRGB [20], SENSEI [26], DAMIC [27], and supernova 1987A [17]. The dotted lines correspond to proposed direct detection searches for MCP scattering, while the dashed lines correspond to the forecast sensitivity of direct deflection [30] (including a solar MCP basin [41]). Each of the direct detection lines were shifted taking into account the variable MCP abundance in the $Q - m_{\chi}$ plane.

in the early universe, leading to an irreducible cosmic MCP background. In particular, MCPs can be produced non-thermally via freeze-in, where annihilations and decays of SM states generate a stable density of MCPs. MCP freeze-in is IR-dominated and proceeds until the process is either kinematically disallowed or until the abundance of SM initial states is depleted by the expansion of the universe. For $Q \sim 10^{-11}$, this slow accumulation of MCPs can account for the observed DM abundance [42–45], providing a target for DM direct detection experiments. At even larger values of Q , the irreducible MCP abundance is larger than the DM abundance, effectively ruling out the parameter space [46]. Meanwhile, for lower values of the millicharge, the MCP background constitutes a small sub-component of the DM. We note that similar arguments have previously been applied to axions and sterile neutrinos [47], as well as real scalars [48], resulting in stringent constraints based on their freeze-in abundance. Notably, axion freeze-in

can be UV-dominated and is sensitive to the reheating temperature of the Universe, whereas sub-MeV MCP freeze-in happens roughly at the same time as Big Bang Nucleosynthesis, regardless of the reheating temperature.

Strikingly, as summarized in Fig. 1, a MCP subcomponent of DM will still be accessible with any DM direct detection searches that have sensitivity to couplings below the freeze-in target, resulting in general bounds on the existence of MCPs regardless of whether they are the DM of our Universe. We find that traditional direct detection searches for MCP-SM scattering (whose sensitivity scales linearly with the MCP density) will be able to constrain a fractional MCP abundance as low as $\sim 10^{-3}$ for keV-TeV masses. Meanwhile, sub-keV MCPs will be most readily accessible to a direct deflection approach (whose sensitivity scales like the MCP density squared), potentially reaching fractional MCP densities eight orders of magnitude below the DM density.

Irreducible MCP Density.— For sub-MeV masses we extend the freeze-in calculation of Ref. [45] to arbitrary abundances, including sub-keV MCP masses. The production of sub-MeV MCPs occurs via two main interactions: the annihilation of electron-positron pairs, $e^+e^- \rightarrow \bar{\chi}\chi$ [49, 50] and the in-medium decay of plasmons [45, 51]. The abundance of MCPs can then be calculated by solving the Boltzmann equation,

$$sHx \frac{dY_\chi}{dx} = 2 \left(n_e^2 \langle \sigma v \rangle_{e^+e^- \rightarrow \bar{\chi}\chi} + n_{\gamma^*} \langle \Gamma \rangle_{\gamma^* \rightarrow \bar{\chi}\chi} \right) \quad (2)$$

where $Y_\chi = n_\chi/s$ is the comoving MCP number density, H is the Hubble rate, s is the entropy density, $x = m_\chi/T$, and the two terms on the right are the thermally-averaged annihilation and plasmon decay rates, respectively. The factor of 2 accounts for the abundance of both χ and $\bar{\chi}$. We do not include a term that captures the backreaction of MCP annihilation or coalescence into SM particles, as we have explicitly checked that the number density of MCPs is always highly suppressed compared to that of SM particles during freeze-in.

MCP production via annihilation occurs until $T \sim \max(m_e, m_\chi)$, corresponding to temperatures when the electrons either freeze-out of the thermal bath or lack sufficient energy to produce MCPs. On the other hand, plasmon decay remains active until the effective plasmon mass (which is similar to the plasma frequency ω_p) drops below twice the MCP mass. At early times $T \gtrsim 1$ MeV, the plasma is relativistic so $\omega_p \approx eT/3$, whereas for $T \lesssim 1$ MeV the plasma frequency depends primarily on the ambient electron density $\omega_p^2 \approx e^2 n_e / m_e$. For sufficiently low-mass MCPs, this means that production occurs in a regime where the chemical potential of electrons μ_e cannot be neglected. We therefore include the electron chemical potential in our calculations, which we obtain by equating the net electron density to the baryon density at all times. At late times when the plasma is nonrelativistic, we find that the electron chemical potential can

be approximated as

$$\mu_e = T \sinh^{-1} \left[\eta \frac{\zeta(3)}{\pi^2} T^3 e^{\frac{m_e}{T}} \left(\frac{m_e T}{2\pi} \right)^{-3/2} \right], \quad (3)$$

in agreement with other treatments in the literature [52].

Although we solve Eq. (2) numerically, including the effects of finite temperature and chemical potential, the relative contribution of the two channels as a function of temperature can be understood using simple scaling arguments. The rates for both annihilation and plasmon decay scale as $\sim T$ whereas the Hubble rate scales as $\sim T^2$, indicating that freeze-in is most active at the lowest temperatures that are kinematically accessible (or that have a sufficient abundance of SM initial states). It is therefore possible to approximate freeze-in as happening at a particular temperature to compute the yield using the relevant collision term in the Boltzmann equation. For e^+e^- annihilation, $\langle \sigma v \rangle n_e^2 \sim e^4 Q^2 T^4$ and the lowest temperature where the process is active is $T \sim \max(m_\chi, m_e)$, giving a comoving MCP abundance that scales as

$$Y_\chi^{e^+e^-} = 1 \times 10^{-9} \left(\frac{Q}{10^{-12}} \right)^2 \left(\frac{1 \text{ MeV}}{\max(m_\chi, m_e)} \right). \quad (4)$$

On the other hand, the plasmon decay term scales as $\langle \Gamma \rangle_{\gamma^* \rightarrow \bar{\chi}\chi} n_{\gamma^*} \sim e^2 Q^2 \omega_p T^3$. As the temperature of the universe decreases, the plasma frequency decreases with a non-trivial scaling (shown as an inset plot in Figure 2), quenching the plasmon decay channel at a characteristic temperature that depends on m_χ . For MCPs above a mass of $m_\chi \gtrsim 10$ keV, plasmon decay ceases at the kinematic threshold, $\omega_p(T) \sim 2m_\chi$. For a ~ 10 keV MCP, this threshold occurs at $T \sim 0.2$ MeV, when the plasma is still fairly relativistic. This results in a comoving abundance,

$$Y_\chi^{\gamma^*} = 2 \times 10^{-10} \left(\frac{Q}{10^{-12}} \right)^2 \left(\frac{1 \text{ MeV}}{m_\chi} \right) \quad \text{if } m_\chi \gtrsim 10 \text{ keV}. \quad (5)$$

For MCPs with lower masses, MCP production is still kinematically allowed during electron freeze-out, which results in an exponential suppression of the plasma frequency. In this case, the electron depletion is primarily responsible for quenching plasmon decay. The production of the MCP background is therefore completed by $T \sim 0.1$ MeV at the very latest, just before the strong exponential suppression of the electron density, regardless of MCP mass or production channel. This results in a comoving MCP abundance proportional to

$$Y_\chi^{\gamma^*} = 3 \times 10^{-8} \left(\frac{Q}{10^{-12}} \right)^2 \quad \text{if } m_\chi \lesssim 10 \text{ keV}, \quad (6)$$

in agreement with Ref. [51]. Eqs. (4)-(6) make it apparent that when $m_\chi \gtrsim 100$ keV, the electron-positron annihilation rate dominates over plasmon decay. Consequently, the total MCP abundance, $\Omega_{\text{MCP}} = m_\chi (Y_{e^+e^-} +$

$Y_{\gamma^*} s_0/\rho_0^c$ scales as $\Omega_{\text{MCP}} \sim Q^2$ for $m_\chi \gtrsim 10$ keV and as $\Omega_{\text{MCP}} \sim Q^2 m_\chi$ for $m_\chi \lesssim 10$ keV, reproducing the scaling seen in Fig. 1.

For MCP masses $m_\chi \gg 1$ MeV, freeze-in production primarily happens through SM fermions $f\bar{f} \rightarrow \chi\bar{\chi}$, as calculated in Ref. [43]. We ignore the effect of Fermi-Dirac statistics, which can shift lines of constant relic abundance by $O(10\%)$ [53]. Since the abundance through these channels is proportional to Q^2 , one can straightforwardly generalize these results to arbitrary values of Q with a simple rescaling, $\Omega_{\text{MCP}} = \Omega_{\text{DM}}(Q/Q_{\text{DM}})^2$, where Q_{DM} is the millicharge required to produce the observed DM abundance Ω_{DM} . Note that at energies near or above the electroweak scale, MCPs additionally couple to the SM Z -boson [54]. Consequently, MCPs in the mass range $1\text{GeV} \lesssim m_\chi \lesssim m_Z/2$ are produced through the decay channel $Z \rightarrow \chi\bar{\chi}$, resulting in the drop in Q required for a fixed abundance as computed in Ref. [53]. Note that the same finite-temperature effects that result in modified photon mixing properties can also affect the Z . However, these corrections are expected to be very small [55, 56], and therefore should not substantially impact our result. For $m_\chi \gtrsim 200$ GeV, production will dominantly happen before the electroweak phase transition, where finite-temperature effects may require a more careful treatment beyond the scope of this work.

Our calculations of the MCP abundance are subject to the caveat that the MCPs cannot be substantially depleted after their production. Notably, the presence of an ultralight A' in the spectrum implies that the MCP abundance can be depleted through $\chi\bar{\chi} \rightarrow A'A'$. Since this process scales as g_χ^4 , it can potentially be efficient despite the sub-thermal abundance of MCPs. Ensuring that this process is always inefficient implies that our calculations are valid when $g_\chi < 3 \times 10^{-4} \times (m_\chi/1\text{ MeV})^{1/2} (\Omega_{\text{DM}}/\Omega_{\text{MCP}})^{1/4}$. Small values of the dark gauge coupling, combined with the freeze-in values of Q and implied kinetic mixing parameter κ may be bolstered by UV considerations [57, 58]. This bound on the dark gauge coupling is also similar to the one obtained through constraints on self-interacting DM (SIDM) that apply when MCPs are assumed to make up all of the dark matter [59, 60]. We finally note that it is possible to entirely avoid the depletion of MCPs by considering the “pure” millicharge case where the MCPs have a small SM hypercharge and thus have a direct coupling to the SM photon. In this case, the only annihilation channel $\chi\bar{\chi} \rightarrow \gamma\gamma$ is suppressed like Q^4 and is therefore safely neglected in the entire parameter space.

Experimental Reach.— By accounting for the variable relic abundance of MCPs in the $Q - m_\chi$ plane, we can recast existing forecasts and constraints that assume MCPs are all of the DM into constraints and forecasts on the mere existence of MCPs. Smaller abundances of MCPs correspond to reduced overall experimental sensitivity due to the reduced flux of particles passing through the detector. We assume that MCPs produced in the early universe have the same gravitational clustering dy-

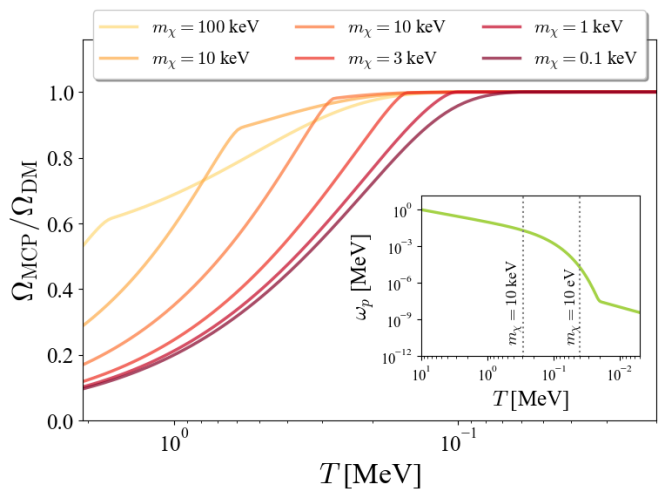


FIG. 2. Evolution of the relic MCP abundance for several MCP masses with values of Q chosen such that $\Omega_{\text{MCP}} = \Omega_{\text{DM}}$. The curves converge at lower MCP masses, where plasmon decay becomes inefficient at $T \sim 0.1$ MeV primarily due to the exponentially falling plasma frequency (shown in the inset) rather than due to the kinematic threshold $\omega_p > 2m_\chi$ (illustrated with vertical dotted lines for two choices of m_χ). MCP production is thus complete by $T \sim 0.1$ MeV at the very latest, regardless of the MCP mass.

namics as the DM, which would imply that the local MCP density corresponds to the rescaled DM density,

$$\rho_{\text{MCP}}(Q, m_\chi) = \rho_{\text{DM}} \frac{\Omega_{\text{MCP}}(Q, m_\chi)}{\Omega_{\text{DM}}} \quad (7)$$

where $\rho_{\text{DM}} \sim 0.3$ GeV/cm³ is the local mass density of DM in the Milky Way [61, 62]. We also assume the MCP background has the same velocity distribution as the DM for similar reasons (most often, direct detection analyses are performed assuming a Maxwellian distribution). To be consistent with these assumptions about the local MCP density and phase space, we only consider MCP masses above ~ 1 eV, since even lighter MCPs would have still have substantial free-streaming velocities at the present day (MCPs lighter than $\sim 10^{-4}$ eV would still be relativistic).

Ongoing and proposed sub-GeV direct detection experiments provide a key avenue for constraining the irreducible MCP background at intermediate MCP masses. Existing analyses and forecasts for these experiments place a bound on the electron scattering cross-section,

$$\bar{\sigma}_e = \frac{16\pi\alpha^2 Q^2 \mu_{\chi e}^2}{(\alpha m_e)^4}, \quad (8)$$

as a function of m_χ (where $\mu_{\chi e}$ is the MCP-electron reduced mass) under the assumption that MCPs make all of the DM. The event rate at these experiments, which determines their sensitivity, scales as $R \propto \rho_{\text{DM}} \bar{\sigma}_e / m_{\text{DM}}$. For the MCP background, we can therefore interpret existing limits on $\bar{\sigma}_e$ as limits on $\bar{\sigma}_e \times (\rho_{\text{MCP}}/\rho_{\text{DM}})$, which can be straightforwardly projected onto the $Q - m_\chi$ plane.

For heavier MCP masses, the experimental program targeting weakly interacting massive particles (WIMPs) via nuclear recoils can be repurposed to search for MCPs. In the mass range $m_\chi \gtrsim \text{GeV}$, MCPs can be detected via their interaction with the protons in the target nucleus. Generally, bounds on the DM-proton cross section assume a heavy A' such that σ_p is suppressed by $m_{A'}^{-4}$. However these bounds can be reinterpreted for the case of an ultralight A' or a “pure” millicharge, resulting in an enhancement at low recoil energies,

$$\sigma_p = \frac{16\pi\alpha^2 Q^2 \mu_{\chi p}^2}{(2m_N E_R)^2} \quad (9)$$

where $\mu_{\chi p}^2$ is the MCP-proton reduced mass, m_N is the mass of the target nucleus, and E_R is the recoil energy. Despite the fact that the differential event rate for a fixed DM mass is different for heavy and light mediators, Ref. [63] pointed out that the two differential event rates can be similar for *distinct* DM masses. Therefore constraints assuming a heavy mediator can be reinterpreted as constraints on MCPs (including the fractional abundance of Eq. (7)) by ensuring that the differential event rates are the same in the two cases [63].

New detection strategies, such as direct deflection [30], are necessary to access sub-keV MCP parameter space. Notably, it would be challenging to detect energy deposition from single-particle scattering at the ~ 1 meV scale, corresponding to a keV-mass particle orbiting in the MW. Direct deflection assumes that the “MCP wind” passing through earth acts like a continuum, and the signal arises due to the collective deflection of the entire wind in an oscillating background electric field, which sources an alternating millicharge electric field downstream of the deflector. The millicharge-induced electric field scales as $E_\chi \sim \rho_{\text{MCP}} Q^2 / m_\chi^2$, and the signal power integrated over the shielded detector region scales as $E_\chi^2 \sim \rho_{\text{MCP}}^2 (Q/m_\chi)^4$. We can thus appropriately rescale the sensitivity of DM searches using direct deflection to searches for MCP states in the spectrum. The same direct deflection setup would also be sensitive to the MCPs generated by the Sun that are trapped in the Solar basin [41]. The sensitivity to the Solar basin MCPs is stronger due to the higher local number density and slower kinematics of basin-generated MCPs compared to frozen-in MCPs.

Astrophysical and Cosmological Constraints.— The overproduction bound shown in Fig. 1 can be understood as the parameter space where the abundance of MCPs produced via freeze-in would be larger than the observed abundance of DM, as discussed in Ref. [46] (or e.g. Ref. [64] in the case of scalars). We note that this overproduction bound is alleviated for $g_\chi \gtrsim 10^{-4}$ when MCP annihilation to dark photons becomes efficient, which opens up the parameter space. Furthermore, throughout this work, we have assumed that the reheating temperature of the Universe is much larger than any of the other relevant temperature scales. However, non-standard early-Universe scenarios could result in lower

reheating temperatures that are constrained by observation to be at least ~ 10 MeV [65–67]. The vertical line in Fig. 1 shows the approximate parameter space where we expect this assumption to affect our calculation. Lowering the reheat temperature could alleviate the overproduction bound for heavy MCPs, as discussed in Ref. [46]. Additionally, frozen-in MCPs never have a thermal abundance and thus never possess substantial entropy, indicating that they do not impact the measured value of N_{eff} , in contrast to freeze-out scenarios [46].

There are many methods to constrain MCPs, for instance from anomalous energy loss from stars and supernovae [17, 20]. Direct detection searches would provide complementary constraints in the low-mass parameter space, which is particularly important since stellar magnetic fields could trap MCPs in stars, in violation of the assumptions typically made in setting stellar energy-loss constraints. Dedicated work is required to understand magnetic trapping in stars, but studies of the Sun suggest that parameter space above $Q \gtrsim 10^{-11}$ could be impacted [68]. Additionally, if MCPs are assumed to make up all of the DM, they can leave imprints in many astrophysical environments. For instance, the initial phase space distribution from freeze-in production can result in suppressed structure formation on small scales [69]. Non-trivial MCP magneto-hydrodynamics may also affect the internal properties of galaxies and galaxy clusters [70–72], particularly accounting for ambient magnetic fields and supernova remnant shocks that may alter the local density and phase-space distribution of MCPs in our Galaxy [73–77]. However, fully characterizing these dark plasma effects (including possible screening due to a finite dark photon mass) remains a challenging problem. The scattering of frozen-in MCPs with baryons can also affect the cosmic microwave background [69] and the 21 cm global signal [78–81]. We expect that these effects will be significantly diminished if MCPs are a small fraction of the total DM abundance. For instance, it has been shown that MCP fractions less than 0.4% cannot be constrained from DM-baryon scattering in the CMB [82] (assuming cold initial conditions). We finally note that fermionic MCPs will not be subject to bounds from Pauli blocking in dwarf galaxies (see e.g. Ref. [83]) if they only constitute a small DM fraction.

Conclusions.— MCPs arise as parts of minimal dark sectors that are weakly coupled to the SM. If MCPs exist in nature, they may not constitute a substantial fraction of the DM. Regardless, in this work we have shown that DM direct detection experiments are sensitive to the existence of MCPs (even if they are a tiny sub-fraction of DM) due to the irreducible MCP density produced in the early universe. In the context of freeze-in production, smaller couplings result in smaller DM fractions (this is in contrast to the freeze-out mechanism, where the opposite is true). Thus, any experiment that has sensitivity below the traditional freeze-in target can probe the existence of a frozen-in MCP background. Notably, we find that direct detection experiments will be able to achieve

world-leading sensitivity to MCPs with masses spanning nine orders of magnitude. This sensitivity to dark sectors further motivates the future direct detection program.

Our results are conservative in the sense that we do not include channels for MCP production outside of freeze-in, which would only increase the MCP density and strengthen the experimental reach. For instance, fully non-thermal production channels like misalignment may also contribute substantially to the ambient density of low-mass MCPs [84]. Our results can also be extended to consider other thermal histories, for instance with an initial dark sector abundance [85].

Acknowledgements.— It is a pleasure to thank Asher Berlin, David Dunsby, Rouven Essig, Felix

Kahlhoefer, Yoni Kahn, Tongyan Lin, Nadav Outmezguine, and Nick Rodd for useful conversations and comments on the manuscript. EI was supported in part by a Natural Sciences and Engineering Research Council of Canada (NSERC) Undergraduate Student Research Award USRA-594131-2024. SH was supported in part by the Canadian Institute of Particle Physics Connect Fellowship. EI, SH, and KS acknowledge support from a NSERC Subatomic Physics Discovery Grant, and from the Canada Research Chairs program. KS thanks the Kavli Institute for Theoretical Physics (supported by grant NSF PHY-2309135) for their hospitality during the completion of this work. This analysis made use of Numpy [86], Scipy [87], Matplotlib [88], WebPlotDigitizer [89], Jupyter [90] and Mathematica [91].

-
- [1] C. Boehm and Pierre Fayet, “Scalar dark matter candidates,” *Nucl. Phys. B* **683**, 219–263 (2004), [arXiv:hep-ph/0305261](#).
- [2] Maxim Pospelov, Adam Ritz, and Mikhail B. Voloshin, “Secluded WIMP Dark Matter,” *Phys. Lett. B* **662**, 53–61 (2008), [arXiv:0711.4866 \[hep-ph\]](#).
- [3] Kingman Cheung and Tzu-Chiang Yuan, “Hidden fermion as milli-charged dark matter in Stueckelberg Z-prime model,” *JHEP* **03**, 120 (2007), [arXiv:hep-ph/0701107](#).
- [4] Daniel Feldman, Zuowei Liu, and Pran Nath, “The Stueckelberg Z-prime Extension with Kinetic Mixing and Milli-Charged Dark Matter From the Hidden Sector,” *Phys. Rev. D* **75**, 115001 (2007), [arXiv:hep-ph/0702123](#).
- [5] Eung Jin Chun, Jong-Chul Park, and Stefano Scopel, “Dark matter and a new gauge boson through kinetic mixing,” *JHEP* **02**, 100 (2011), [arXiv:1011.3300 \[hep-ph\]](#).
- [6] Bob Holdom, “Two U(1)’s and Epsilon Charge Shifts,” *Phys. Lett. B* **166**, 196–198 (1986).
- [7] Maxim Pospelov, “Secluded U(1) below the weak scale,” *Phys. Rev. D* **80**, 095002 (2009), [arXiv:0811.1030 \[hep-ph\]](#).
- [8] Marco Fabbrichesi, Emidio Gabrielli, and Gaia Lanfranchi, “The Dark Photon,” (2020), [10.1007/978-3-030-62519-1](#), [arXiv:2005.01515 \[hep-ph\]](#).
- [9] Keith R. Dienes, Christopher F. Kolda, and John March-Russell, “Kinetic mixing and the supersymmetric gauge hierarchy,” *Nucl. Phys. B* **492**, 104–118 (1997), [arXiv:hep-ph/9610479](#).
- [10] S. A. Abel, M. D. Goodsell, J. Jaeckel, V. V. Khoze, and A. Ringwald, “Kinetic Mixing of the Photon with Hidden U(1)s in String Phenomenology,” *JHEP* **07**, 124 (2008), [arXiv:0803.1449 \[hep-ph\]](#).
- [11] Mark Goodsell, Joerg Jaeckel, Javier Redondo, and Andreas Ringwald, “Naturally Light Hidden Photons in LARGE Volume String Compactifications,” *JHEP* **11**, 027 (2009), [arXiv:0909.0515 \[hep-ph\]](#).
- [12] Gary Shiu, Pablo Soler, and Fang Ye, “Milli-Charged Dark Matter in Quantum Gravity and String Theory,” *Phys. Rev. Lett.* **110**, 241304 (2013), [arXiv:1302.5471 \[hep-th\]](#).
- [13] Haipeng An, Maxim Pospelov, and Josef Pradler, “Dark Matter Detectors as Dark Photon Helioscopes,” *Phys. Rev. Lett.* **111**, 041302 (2013), [arXiv:1304.3461 \[hep-ph\]](#).
- [14] Haipeng An, Maxim Pospelov, and Josef Pradler, “New stellar constraints on dark photons,” *Phys. Lett. B* **725**, 190–195 (2013), [arXiv:1302.3884 \[hep-ph\]](#).
- [15] Javier Redondo and Georg Raffelt, “Solar constraints on hidden photons re-visited,” *JCAP* **08**, 034 (2013), [arXiv:1305.2920 \[hep-ph\]](#).
- [16] Maurizio Giannotti, Igor Irastorza, Javier Redondo, and Andreas Ringwald, “Cool WISPs for stellar cooling excesses,” *JCAP* **05**, 057 (2016), [arXiv:1512.08108 \[astro-ph.HE\]](#).
- [17] Jae Hyeok Chang, Rouven Essig, and Samuel D. McDermott, “Supernova 1987A Constraints on Sub-GeV Dark Sectors, Millicharged Particles, the QCD Axion, and an Axion-like Particle,” *JHEP* **09**, 051 (2018), [arXiv:1803.00993 \[hep-ph\]](#).
- [18] Robert Lasenby and Ken Van Tilburg, “Dark photons in the solar basin,” *Phys. Rev. D* **104**, 023020 (2021), [arXiv:2008.08594 \[hep-ph\]](#).
- [19] Matthew J. Dolan, Frederick J. Hiskens, and Raymond R. Volkas, “Constraining dark photons with self-consistent simulations of globular cluster stars,” *JCAP* **05**, 099 (2024), [arXiv:2306.13335 \[hep-ph\]](#).
- [20] Audrey Fung, Saniya Heeba, Qinrui Liu, Varun Muralidharan, Katelin Schutz, and Aaron C. Vincent, “New bounds on light millicharged particles from the tip of the red-giant branch,” *Phys. Rev. D* **109**, 083011 (2024), [arXiv:2309.06465 \[hep-ph\]](#).
- [21] Asher Berlin, Nikita Blinov, Gordan Krnjaic, Philip Schuster, and Natalia Toro, “Dark Matter, Millicharges, Axion and Scalar Particles, Gauge Bosons, and Other New Physics with LDMX,” *Phys. Rev. D* **99**, 075001 (2019), [arXiv:1807.01730 \[hep-ph\]](#).
- [22] Torsten Åkesson *et al.* (LDMX), “Light Dark Matter experiment (LDMX),” (2018), [arXiv:1808.05219 \[hep-ex\]](#).
- [23] Philip Ilten, Yotam Soreq, Mike Williams, and Wei Xue, “Serendipity in dark photon searches,” *JHEP* **06**, 004 (2018), [arXiv:1801.04847 \[hep-ph\]](#).
- [24] Juliette Alimena *et al.*, “Searching for long-lived particles beyond the Standard Model at the Large Hadron Collider,” *J. Phys. G* **47**, 090501 (2020), [arXiv:1903.04497 \[hep-ex\]](#).
- [25] N. Aghanim *et al.* (Planck), “Planck2018 results: Vi. cos-

- mological parameters,” *Astronomy & Astrophysics* **641**, A6 (2020).
- [26] Prakruth Adari *et al.* (SENSEI), “SENSEI: First Direct-Detection Results on sub-GeV Dark Matter from SENSEI at SNOLAB,” (2023), [arXiv:2312.13342 \[astro-ph.CO\]](#).
- [27] I. Arnquist *et al.* (DAMIC-M), “First Constraints from DAMIC-M on Sub-GeV Dark-Matter Particles Interacting with Electrons,” *Phys. Rev. Lett.* **130**, 171003 (2023), [arXiv:2302.02372 \[hep-ex\]](#).
- [28] Alexis Aguilar-Arevalo *et al.* (Oscura), “The Oscura Experiment,” (2022), [arXiv:2202.10518 \[astro-ph.IM\]](#).
- [29] Simon Knapen, Tongyan Lin, and Kathryn M. Zurek, “Light Dark Matter: Models and Constraints,” *Phys. Rev. D* **96**, 115021 (2017), [arXiv:1709.07882 \[hep-ph\]](#).
- [30] Asher Berlin, Raffaele Tito D’Agnolo, Sebastian A. R. Ellis, Philip Schuster, and Natalia Toro, “Directly Deflecting Particle Dark Matter,” *Phys. Rev. Lett.* **124**, 011801 (2020), [arXiv:1908.06982 \[hep-ph\]](#).
- [31] Simon Knapen, Tongyan Lin, Matt Pyle, and Kathryn M. Zurek, “Detection of Light Dark Matter With Optical Phonons in Polar Materials,” *Phys. Lett. B* **785**, 386–390 (2018), [arXiv:1712.06598 \[hep-ph\]](#).
- [32] Sinead Griffin, Simon Knapen, Tongyan Lin, and Kathryn M. Zurek, “Directional Detection of Light Dark Matter with Polar Materials,” *Phys. Rev. D* **98**, 115034 (2018), [arXiv:1807.10291 \[hep-ph\]](#).
- [33] Brian Campbell-Deem, Simon Knapen, Tongyan Lin, and Ethan Villarama, “Dark matter direct detection from the single phonon to the nuclear recoil regime,” *Phys. Rev. D* **106**, 036019 (2022), [arXiv:2205.02250 \[hep-ph\]](#).
- [34] Connor Stratman Tongyan Lin, personal communication.
- [35] S Derenzo, W Guo, S Hertel, P Sorensen, A Suzuki, and K Zurek, “Snowmass2021-letter of interest the tesseract dark matter project,” (2021).
- [36] Yonit Hochberg, Yonatan Kahn, Mariangela Lisanti, Kathryn M. Zurek, Adolfo G. Grushin, Roni Ilan, Sinéad M. Griffin, Zhen-Fei Liu, Sophie F. Weber, and Jeffrey B. Neaton, “Detection of sub-MeV Dark Matter with Three-Dimensional Dirac Materials,” *Phys. Rev. D* **97**, 015004 (2018), [arXiv:1708.08929 \[hep-ph\]](#).
- [37] R. Matthias Geilhufe, Felix Kahlhoefer, and Martin Wolfgang Winkler, “Dirac materials for sub-meV dark matter detection: New targets and improved formalism,” *Physical Review D* **101** (2020), [10.1103/physrevd.101.055005](#).
- [38] Peizhi Du, Daniel Egaña Ugrinovic, Rouven Essig, and Mukul Sholapurkar, “Doped semiconductor devices for sub-MeV dark matter detection,” *Phys. Rev. D* **109**, 055009 (2024), [arXiv:2212.04504 \[hep-ph\]](#).
- [39] Yonit Hochberg, Yonatan Kahn, Noah Kurinsky, Benjamin V. Lehmann, To Chin Yu, and Karl K. Berggren, “Determining Dark-Matter–Electron Scattering Rates from the Dielectric Function,” *Phys. Rev. Lett.* **127**, 151802 (2021), [arXiv:2101.08263 \[hep-ph\]](#).
- [40] Simon Knapen, Jonathan Kozacuk, and Tongyan Lin, “Dark matter-electron scattering in dielectrics,” *Phys. Rev. D* **104**, 015031 (2021), [arXiv:2101.08275 \[hep-ph\]](#).
- [41] Asher Berlin and Katelin Schutz, “Helioscope for gravitationally bound millicharged particles,” *Phys. Rev. D* **105**, 095012 (2022), [arXiv:2111.01796 \[hep-ph\]](#).
- [42] Jedamzik K. March-Russell J. et al. Hall, L.J., “Freeze-in production of FIMP dark matter,” *J. High Energ. Phys.* **80** (2010), [10.1007/JHEP03\(2010\)080](#).
- [43] Xiaoyong Chu, Thomas Hambye, and Michel H. G. Tytgat, “The Four Basic Ways of Creating Dark Matter Through a Portal,” *JCAP* **05**, 034 (2012), [arXiv:1112.0493 \[hep-ph\]](#).
- [44] Nicolás Bernal, Matti Heikinheimo, Tommi Tenkanen, Kimmo Tuominen, and Ville Vaskonen, “The dawn of fimp dark matter: A review of models and constraints,” *International Journal of Modern Physics A* **32**, 1730023 (2017), [https://doi.org/10.1142/S0217751X1730023X](#).
- [45] Cora Dvorkin, Tongyan Lin, and Katelin Schutz, “Making dark matter out of light: Freeze-in from plasma effects,” *Physical Review D* **99** (2019), [10.1103/physrevd.99.115009](#).
- [46] Xucheng Gan and Yu-Dai Tsai, “Cosmic Millicharge Background and Reheating Probes,” (2023), [arXiv:2308.07951 \[hep-ph\]](#).
- [47] Kevin Langhoff, Nadav Joseph Outmezguine, and Nicholas L. Rodd, “Irreducible axion background,” *Physical Review Letters* **129** (2022), [10.1103/physrevlett.129.241101](#).
- [48] Francesco D’Eramo, Andrea Tesi, and Ville Vaskonen, “Irreducible cosmological backgrounds of a real scalar with a broken symmetry,” (2024), [arXiv:2407.19997 \[hep-ph\]](#).
- [49] Rouven Essig, Jeremy Mardon, and Tomer Volansky, “Direct detection of sub-gev dark matter,” *Phys. Rev. D* **85**, 076007 (2012).
- [50] Rouven Essig, Aaron Manalaysay, Jeremy Mardon, Peter Sorensen, and Tomer Volansky, “First direct detection limits on sub-gev dark matter from xenon10,” *Phys. Rev. Lett.* **109**, 021301 (2012).
- [51] Asher Berlin, Jeff A. Dror, Xucheng Gan, and Joshua T. Ruderman, “Millicharged relics reveal massless dark photons,” *JHEP* **05**, 046 (2023), [arXiv:2211.05139 \[hep-ph\]](#).
- [52] Luke C. Thomas, Ted Dezen, Evan B. Grohs, and Chad T. Kishimoto, “Electron-positron annihilation freeze-out in the early universe,” *Physical Review D* **101** (2020), [10.1103/physrevd.101.063507](#).
- [53] Saniya Heeba, Tongyan Lin, and Katelin Schutz, “Inelastic freeze-in,” *Phys. Rev. D* **108**, 095016 (2023), [arXiv:2304.06072 \[hep-ph\]](#).
- [54] Jared A. Evans, Stefania Gori, and Jessie Shelton, “Looking for the WIMP Next Door,” *JHEP* **02**, 100 (2018), [arXiv:1712.03974 \[hep-ph\]](#).
- [55] D. Comelli and J. R. Espinosa, “Bosonic thermal masses in supersymmetry,” *Phys. Rev. D* **55**, 6253–6263 (1997).
- [56] Saniya Heeba and Felix Kahlhoefer, “Probing the freeze-in mechanism in dark matter models with U(1) gauge extensions,” *Phys. Rev. D* **101**, 035043 (2020), [arXiv:1908.09834 \[hep-ph\]](#).
- [57] Matthew Reece, “Photon Masses in the Landscape and the Swampland,” *JHEP* **07**, 181 (2019), [arXiv:1808.09966 \[hep-th\]](#).
- [58] Tony Gherghetta, Jörn Kersten, Keith Olive, and Maxim Pospelov, “Evaluating the price of tiny kinetic mixing,” *Phys. Rev. D* **100**, 095001 (2019), [arXiv:1909.00696 \[hep-ph\]](#).
- [59] Sean Tulin and Hai-Bo Yu, “Dark Matter Self-interactions and Small Scale Structure,” *Phys. Rept.* **730**, 1–57 (2018), [arXiv:1705.02358 \[hep-ph\]](#).
- [60] Janis Kummer, Marcus Brüggen, Klaus Dolag, Felix Kahlhoefer, and Kai Schmidt-Hoberg, “Simulations of core formation for frequent dark matter self-interactions,” *Mon. Not. Roy. Astron. Soc.* **487**, 354–363

- (2019), [arXiv:1902.02330 \[astro-ph.CO\]](#).
- [61] J. I. Read, “The Local Dark Matter Density,” *J. Phys. G* **41**, 063101 (2014), [arXiv:1404.1938 \[astro-ph.GA\]](#).
- [62] Pablo F. de Salas and Axel Widmark, “Dark matter local density determination: recent observations and future prospects,” *Rept. Prog. Phys.* **84**, 104901 (2021), [arXiv:2012.11477 \[astro-ph.GA\]](#).
- [63] Thomas Hambye, Michel H. G. Tytgat, Jérôme Vandecasteele, and Laurent Vanderheyden, “Dark matter direct detection is testing freeze-in,” *Phys. Rev. D* **98**, 075017 (2018), [arXiv:1807.05022 \[hep-ph\]](#).
- [64] Oleg Lebedev, “Scalar overproduction in standard cosmology and predictivity of non-thermal dark matter,” *JCAP* **02**, 032 (2023), [arXiv:2210.02293 \[hep-ph\]](#).
- [65] Takuya Hasegawa, Nagisa Hiroshima, Kazunori Kohri, Rasmus S. L. Hansen, Thomas Tram, and Steen Hannestad, “MeV-scale reheating temperature and thermalization of oscillating neutrinos by radiative and hadronic decays of massive particles,” *JCAP* **12**, 012 (2019), [arXiv:1908.10189 \[hep-ph\]](#).
- [66] P. F. de Salas, M. Lattanzi, G. Mangano, G. Miele, S. Pastor, and O. Pisanti, “Bounds on very low reheating scenarios after Planck,” *Phys. Rev. D* **92**, 123534 (2015), [arXiv:1511.00672 \[astro-ph.CO\]](#).
- [67] Steen Hannestad, “What is the lowest possible reheating temperature?” *Phys. Rev. D* **70**, 043506 (2004), [arXiv:astro-ph/0403291](#).
- [68] Núria Vinyoles and Hendrik Vogel, “Minicharged Particles from the Sun: A Cutting-Edge Bound,” *JCAP* **03**, 002 (2016), [arXiv:1511.01122 \[hep-ph\]](#).
- [69] Cora Dvorkin, Tongyan Lin, and Katelin Schutz, “Cosmology of Sub-MeV Dark Matter Freeze-In,” *Phys. Rev. Lett.* **127**, 111301 (2021), [arXiv:2011.08186 \[astro-ph.CO\]](#).
- [70] Akaxia Cruz and Matthew McQuinn, “Astrophysical plasma instabilities induced by long-range interacting dark matter,” *JCAP* **04**, 028 (2023), [arXiv:2202.12464 \[astro-ph.CO\]](#).
- [71] Albert Stebbins and Gordan Krnjaic, “New Limits on Charged Dark Matter from Large-Scale Coherent Magnetic Fields,” *JCAP* **12**, 003 (2019), [arXiv:1908.05275 \[astro-ph.CO\]](#).
- [72] Robert Lasenby, “Long range dark matter self-interactions and plasma instabilities,” *JCAP* **11**, 034 (2020), [arXiv:2007.00667 \[hep-ph\]](#).
- [73] Leonid Chuzhoy and Edward W. Kolb, “Reopening the window on charged dark matter,” *JCAP* **07**, 014 (2009), [arXiv:0809.0436 \[astro-ph\]](#).
- [74] R. Foot, “Do magnetic fields prevent mirror particles from entering the galactic disk?” *Phys. Lett. B* **699**, 230–232 (2011), [arXiv:1011.5078 \[hep-ph\]](#).
- [75] David Dunskey, Lawrence J. Hall, and Keisuke Harigaya, “CHAMP Cosmic Rays,” *JCAP* **07**, 015 (2019), [arXiv:1812.11116 \[astro-ph.HE\]](#).
- [76] Jung-Tsung Li and Tongyan Lin, “Dynamics of millicharged dark matter in supernova remnants,” *Phys. Rev. D* **101**, 103034 (2020), [arXiv:2002.04625 \[astro-ph.CO\]](#).
- [77] Asher Berlin, Hongwan Liu, Maxim Pospelov, and Harikrishnan Ramani, “Terrestrial density of strongly-coupled relics,” *Phys. Rev. D* **109**, 075027 (2024), [arXiv:2302.06619 \[hep-ph\]](#).
- [78] Asher Berlin, Dan Hooper, Gordan Krnjaic, and Samuel D. McDermott, “Severely constraining dark-matter interpretations of the 21-cm anomaly,” *Phys. Rev. Lett.* **121**, 011102 (2018).
- [79] Rennan Barkana, Anastasia Fialkov, Hongwan Liu, and Nadav Joseph Outmezguine, “Anticipating a new physics signal in upcoming 21-cm power spectrum observations,” *Phys. Rev. D* **108**, 063503 (2023), [arXiv:2212.08082 \[hep-ph\]](#).
- [80] Rennan Barkana, Nadav Joseph Outmezguine, Diego Redigolo, and Tomer Volansky, “Strong constraints on light dark matter interpretation of the EDGES signal,” *Phys. Rev. D* **98**, 103005 (2018), [arXiv:1803.03091 \[hep-ph\]](#).
- [81] Hongwan Liu, Nadav Joseph Outmezguine, Diego Redigolo, and Tomer Volansky, “Reviving Millicharged Dark Matter for 21-cm Cosmology,” *Phys. Rev. D* **100**, 123011 (2019), [arXiv:1908.06986 \[hep-ph\]](#).
- [82] Kimberly K. Boddy, Vera Gluscevic, Vivian Poulin, Ely D. Kovetz, Marc Kamionkowski, and Rennan Barkana, “Critical assessment of CMB limits on dark matter-baryon scattering: New treatment of the relative bulk velocity,” *Phys. Rev. D* **98**, 123506 (2018), [arXiv:1808.00001 \[astro-ph.CO\]](#).
- [83] James Alvey, Nashwan Sabti, Victoria Tiki, Diego Blas, Kyrlo Bondarenko, Alexey Boyarsky, Miguel Escudero, Malcolm Fairbairn, Matthew Orkney, and Justin I. Read, “New constraints on the mass of fermionic dark matter from dwarf spheroidal galaxies,” *Mon. Not. Roy. Astron. Soc.* **501**, 1188–1201 (2021), [arXiv:2010.03572 \[hep-ph\]](#).
- [84] Zachary Bogorad and Natalia Toro, “Ultralight millicharged dark matter via misalignment,” *JHEP* **07**, 035 (2022), [arXiv:2112.11476 \[hep-ph\]](#).
- [85] Nicolas Fernandez, Yonatan Kahn, and Jessie Shelton, “Freeze-in, glaciation, and UV sensitivity from light mediators,” *JHEP* **07**, 044 (2022), [arXiv:2111.13709 \[hep-ph\]](#).
- [86] Charles R Harris, K Jarrod Millman, Stéfan J Van Der Walt, Ralf Gommers, Pauli Virtanen, David Cournapeau, Eric Wieser, Julian Taylor, Sebastian Berg, Nathaniel J Smith, *et al.*, “Array programming with numpy,” *Nature* **585**, 357–362 (2020).
- [87] Pauli Virtanen, Ralf Gommers, Travis E Oliphant, Matt Haberland, Tyler Reddy, David Cournapeau, Evgeni Burovski, Pearu Peterson, Warren Weckesser, Jonathan Bright, *et al.*, “Scipy 1.0: fundamental algorithms for scientific computing in python,” *Nature methods* **17**, 261–272 (2020).
- [88] John D Hunter, “Matplotlib: A 2d graphics environment,” *Computing in science & engineering* **9**, 90–95 (2007).
- [89] A Rohatgi, “Webplotdigitizer,” (2018).
- [90] Thomas Kluyver *et al.*, “Jupyter notebooks a publishing format for reproducible computational workflows,” in *Positioning and Power in Academic Publishing: Players, Agents and Agendas* (IOS Press, 2016) pp. 87–90.
- [91] Stephen Wolfram, *The mathematica book* (Wolfram Research, Inc., 2003).